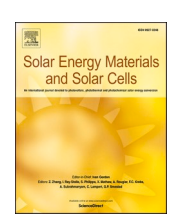
ELSEVIER

Contents lists available at ScienceDirect

Solar Energy Materials and Solar Cells

journal homepage: www.elsevier.com/locate/solmat





Accelerating the hydration reaction of potassium carbonate using organic dopants

Jelle Houben^a, Joris van Biesen^a, Henk Huinink^{a,b,*}, Hartmut R. Fischer^c, Olaf C.G. Adan^{a,c}

- ^a Eindhoven University of Technology, Den Dolech 2, 5600 MB, Eindhoven, the Netherlands
- ^b EIRES, Horsten 1, 5612 AX, Eindhoven, the Netherlands
- ^c TNO Materials Solutions, High Tech Campus 25, 5656 AE, Eindhoven, the Netherlands

ARTICLE INFO

Keywords: Organic potassium salt doping Potassium carbonate Potassium formate Potassium acetate Surface mobility

ABSTRACT

Potassium carbonate has recently been identified as a promising candidate for thermochemical energy storage. However, as for many salt hydrates, the reaction kinetics is limited, and moreover, the hydration transition is kinetically hindered due to a metastable zone, involving limited mobility. This work aims to improve mobility by using organic potassium dopants, it shows that doping with potassium-formate and -acetate, can accelerate the hydration reaction. It has been shown that these dopants can enhance the hydration rate by two mechanisms i.e. introducing mobility due to adsorption of more water or introducing more surface area, where water adsorption can occur. This work opens up new possibilities for organic dopants to enhance the performance of salt hydrates.

1. Introduction

Significant growth in the global population has put a heavy load on fossil fuels and by their abundant use creating a threat of climate change. This threat is recognized in the Paris Agreement of 2015 and agreed to reduce greenhouse gas emissions to 80–95% below 1990 levels by 2050 [1]. To reduce the GHG emissions, a transition from fossil fuels to renewable energies has to be made. Solar energy is regarded as one of the most promising renewable energy sources [2].

The development of efficient energy systems is one of the main challenges to make the transition from a fossil based energy society to a renewable based energy society. To increase energy efficiency, the production of energy should be as close as possible to the end user, thereby mitigating conversion and transport losses. These decentralized energy options include combined heat and power, district heating and cooling, geothermal, biomass and solar energy [3]. For these decentralized systems, energy storage is a necessity to match demand and supply in time and power. Storage is particularly crucial for thermal energy systems based on solar energy. Solar energy, like other renewable energy sources, is characterized by its intermittent behaviour. This originates from the variations in solar irradiation with the weather, location, time and season of the year [4]. Therefore, advanced energy storage is a crucial technology for a widespread integration of renewable energies in our total energy supply.

Thermochemical energy storage is a promising candidate for advanced energy storage, as it offers a high energy storage density (ESD, specific ther-mal storage capacity, 0.22–2.79 GJ/m³ [5]) and negligible heat loss [6,7].

Thermochemical heat storage works on the basis of reversible sorption re-actions, which are used to store energy. Sorption is defined as the fixation or capture of a gas (called sorbate) by a solid or liquid (called sorbent) [8]. Salt hydrates are a promising subclass of thermochemical storage materials, as they offer a high energy density, operation temperatures suitable for the built environment and use water vapour as sorbate, which is inherently safe and environmentally friendly) [9]. From an extensive review of 563 hydrate reactions, potassium carbonate (K_2CO_3) has been selected as one of the most promising materials for domestic heat storage based on the temperature op-erating window, stability, price and safety [5].

It has been demonstrated recently by Sögütoglu et al. [10], that a metastable zone (MSZ) exist for K_2CO_3 , which is a near-equilibrium region, where the phase transition is kinetically hindered. This can be described by classical nucleation theory. In Fig. 1 this zone is indicated by the dashed lines above and below the equilibrium lines of K_2CO_3 . In the work of Sögütoglu et al. [10] it is hypothesized that the hydration reaction is a transition mo-bilized by a wetting layer. The mobility of this wetting layer increases with increasing supersaturation. At the metastable boundary (where noticeable hydration rates start) instantaneous

^{*} Corresponding author. Eindhoven University of Technology, Den Dolech 2, 5600 MB, Eindhoven, the Netherlands. *E-mail address:* h.p.huinink@tue.nl (H. Huinink).

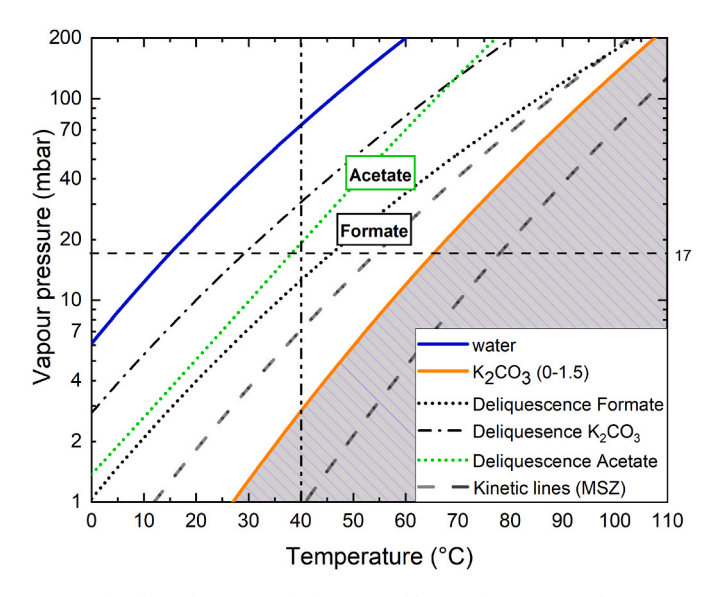


Fig. 1. The phase diagram with the metastable zone for K_2CO_3 . Deliquescence relative humidities of the dopants indicated with respect to the hydration conditions of 17 mbar and 40 °C.

nucleation is expected.

In previous work [11] it has been shown that there is surface mobility already in the MSZ, which increases with increasing water vapour pressure, but not yet sufficient mobility to initiate the phase transition. Sufficient mobility, of water and ions, is only introduced at the MSZ boundary, facilitated by water adsorption. Mobility is therefore a prerequisite for nucleation [11]. In the work of Steiger et al. [12] it has already been shown that if sufficient water is adsorbed, the phase transition occurs via a two-step process, dissolution and subsequent crystallization. Introducing more mobility by adsorbing more water on the surface using highly deliquescent salt has been shown effective in accelerating the hydration reaction of K_2CO_3 [13,14].

Therefore, the aim of this work is to enhance hydration kinetics by in-troducing mobility. This is done using highly soluble organic potassium dopants to adsorb more water on K_2CO_3 to enhance material kinetics. Or-ganic dopants could increase the hydration rate by either, increasing the effective surface area after preparation, or by actively adsorbing more water on the surface prior to hydration. Both increase mobility and thereby en-hance the hydration rate of K_2CO_3 , since ionic mobility is a prerequisite for the phase transition.

2. Material & methods

2.1. Material

2.1.1. Dopant selection

Doping candidates are selected based on three criteria; anion doping, car-boxylate ion, and solubility. Firstly, anion doping is selected since there are numerous potassium salts, which can be screened. In previous work cation ion doping is screened, where the number of candidates was limited [14]. Secondly, organic compounds are selected, since much more candidates are available then in case of inorganic dopants. From the organic compounds, we select organic potassium salts with the carboxylate ion, since there is possibly compatibility with the potassium carbonate lattice, leading to sur-face decoration. The carbonate and carboxylate ion have a similar molecular geometry and the ion size for the carbonate ion, CO_{3}^{-} , is $1.78^{\circ}A$ and for the carboxylate ion, RCO_{2}^{-} , $1.27^{\circ}A$. Electrostatically they will not be compatible, as the carbonate ion has -2 charge and the carboxylate -1. Thirdly, most importantly, the final selection criteria is solubility, since higher-solubility compounds tend to have lower DRH values [15]. This will result in increased

water adsorption on the surface of K₂CO₃.

An overview of candidates is shown in Fig. 2.

2.1.2. Preparation

All samples, including pure potassium carbonate, are prepared via the same method; forced crystallization using an rotary evaporator. All dopants are mixed on powder level at a mol ratio of 1:20. Then the mixed powder is dissolved using demineralized water. The solutions are then transferred to an evaporating flask of a Buchi® Rotavapor R-200. The water bath temperature is set at a temperature of 80 $^{\circ}\text{C}$ with a low pressure conditioned at 60 mbar.

During preparation the flask rotates, thereby creating a thin film in which the salt crystallizes quickly. After crystallization, the powder is post-dried in an oven at 130 $^{\circ}\text{C}$ to remove the bound crystal water. Finally, the dried material is grounded and sieved into a fraction between 50 and 160 μm . Table 1 shows an overview of all doped samples.

2.2. Methods

2.2.1. TGA

All samples are measured isobaric (12 mbar) and isothermally (40 $^{\circ}$ C) in a kinetic screening. This is done using nitrogen as an inert carrier gas for the water vapour. The dehydration time is 4 h and the hydration time is 8 h. Two cycles are measured, the first directly after preparation and the second after 20 hydration dehydration cycles. The cycling is done at 17 mbar and between 40 and 140 $^{\circ}$ C.

2.2.2. SEM

The morphology of the samples is studied using scanning electron mi-croscopy (SEM). For surface analysis, a FEI Quanta 600 FEG field emission scanning electron microscope is used. Images are generated at high vacuum with an acceleration voltage of 2 kV. For elemental analysis of the doped ma-terials a JEOL JSM-IT100 scanning electron microscope is used with energy dispersive spectroscopy (EDS). The analysis is performed at high vacuum with an acceleration voltage of 12 kV.

After crystallization, the powder is post-dried in an oven at 130 $^{\circ}\text{C}.$ After this, the samples are stored and transported in an airtight flask to prevent hydration during storage and transport. The powder (50–160 $\mu\text{m})$ is attached on 12.55 mm aluminum stubs using double sided carbon tape. The sample preparation is done under ambient conditions, but the open-time is minimized (t < 30 s).

2.2.3. BET

The surface area of powder samples is analysed using a Micromeritics $^{\text{TM}}$ Gemini VII surface area analyzer. Sample preparation is done by pre-drying the sample in a FlowPrep $^{\text{TM}}$ sample preparation device, where both heat and a stream of inert gas is used to desorb and remove contaminants. Preparation temperature is 130 °C and purging is done with N_2 .

The sample tube is filled with approximately 4 g sample size and the sample tube is submerged in liquid nitrogen (77.4 K). For the samples, an adsorption/desorption isotherm is measured and a BET analysis is performed at a relative pressure (P/P_0) between 0.05 and 0.30.

3. Results

3.1. Screening

3.1.1. Kinetics

First, all dopant candidates are screened using TGA, with the goal to select the most promising candidates. The screening is done based on hydra-tion kinetics under isobaric and isothermal conditions. Two measurements are performed. The first on material directly after preparation and the second measurement after 20 cycles to validate the cyclic stability of the dopants.

The isobaric and isothermal measurement is performed as follows: at

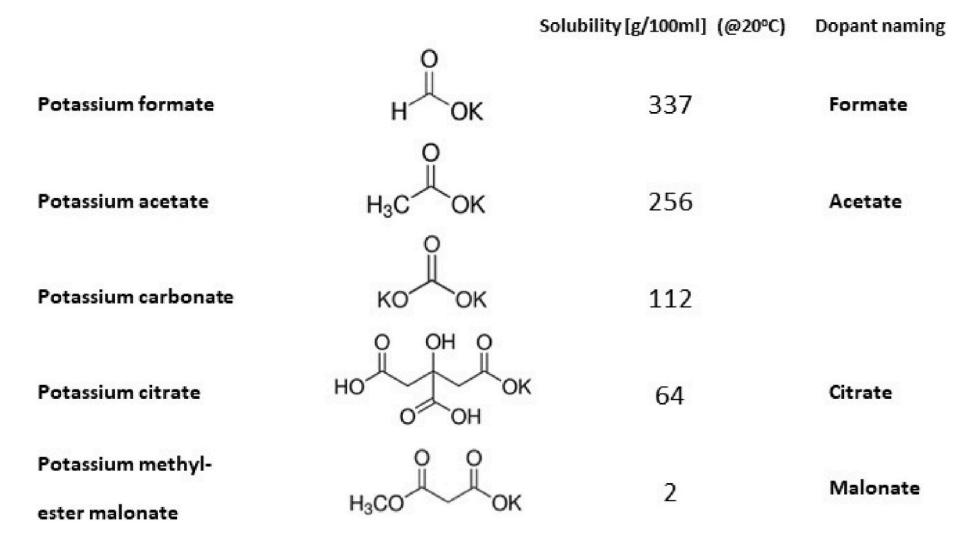


Fig. 2. Overview of doping candidates (and pure K2CO3) with their chemical structure, water solubility and the naming used in this work.

Table 1Overview of dopants, preparation methods and content. The first column represents the dopant concentration in molar ratio, the second column in mass ratio.

Dopant Potassium-	Preparation method	Content [mol x:100]	Content [mass x:100]
Formate	Rotary evaporator	5	3.0
Acetate	Rotary evaporator	5	3.4
Citrate	Rotary evaporator	5	10.0
Malonate	Rotary evaporator	5	5.3

 $t{=}0$ the temperature is set to 140 $^{\circ}\text{C}$, for 3 h to completely dehydrate the sample. At $t{=}3$ h the temperature is switched to 40 $^{\circ}\text{C}$, without supplying water vapour, to equilibrate the sample thermally. Water vapour (17 mbar) is supplied at $t{=}4$ h, to start hydration. This measurement is performed for the samples with dopants according to Figs. 2 and 3 shows the results.

In orange, the hydration of pure K_2CO_3 shows, that the sample is not yet completely hydrated at $12\ h$. Almost all doped samples are fully converted within $1\ h$, all indicating an increase in the hydration kinetics. Potassium citrate does not reach a loading of $1.5\ mol$ water per mol

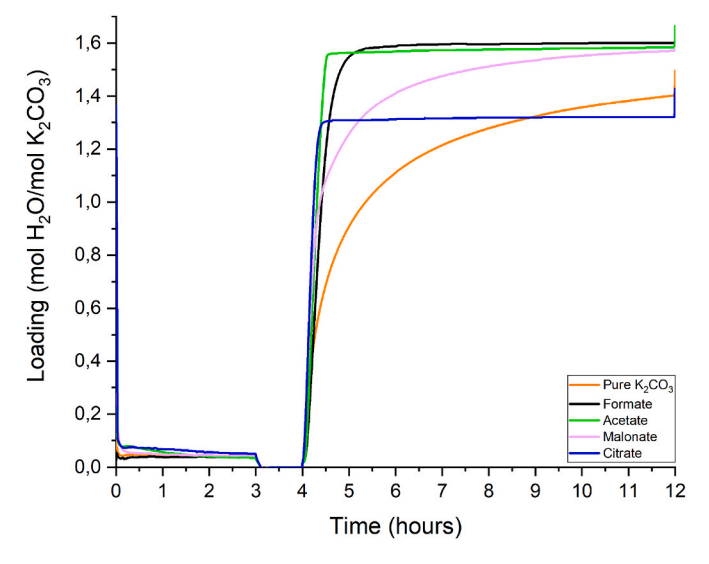


Fig. 3. Isobaric and isothermal hydration measurement for all doped- and pure $K_2\mathrm{CO}_3$. Water vapour (17 mbar) is supplied at t=4 h, where hydration directly starts.

 $\rm K_2CO_3$, as probably a new compound is formed which does not hydrate under the given conditions. Due to this its ill performance this compound has not been further studied.

3.1.2. Stability

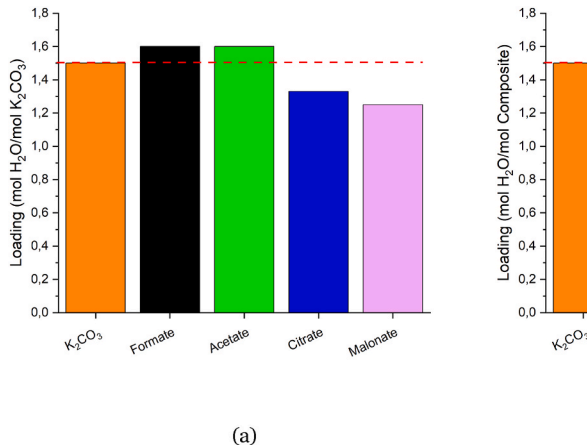
To check the stability of the dopants, samples are cycled 20 times. Fig. 4 shows the end loading after 20 cycles.

Initially, all samples except for potassium citrate reach an end loading above 1.5 mol $\rm H_2O/mol~K_2CO_3$. After 20 cycles, methyl ester malonate does not hydrate completely anymore, indicating that the dopant behaviour is not stable during cycling. Therefore, methyl ester malonate is not further investigated. Moreover, citrate is disregarded as the it does not hydrate completely directly after preparation. In other words, from now on we will limit the discussion to potassium-formate and -acetate.

3.1.3. Dopants water uptake behaviour

To investigate how the dopant affects the hydration behaviour (kinetics and increased loading) of $\rm K_2CO_3$, the pure dopants are hydrated. This is done isobarically with varying temperature, thereby screening for the onset points of water uptake. In this way, the mobility of the adsorbed water adsorption can be analysed [14]. The experiment starts with a dehydration at 140 °C and 17 mbar water vapour pressure. Then, the temperature is decreased with a cooling rate of 1 K/min until 40 °C, followed by temperature increase till 90 °C to dehydrate. After this the temperature is lowered to 40 °C again to re-hydrate the sample, after which the temperature is lowered until deliquescence. The results are shown in Fig. 5. The red line is the sample temperature corresponding to the right y-axis, the other lines are the loading of the different samples, corresponding to the left y-axis. The x-axis is the time in hours.

In Fig. 5 it can be seen that both potassium formate and potassium acetate take up water in the operating window (40 $^{\circ}$ C, 17 mbar), whereby potassium acetate takes up the most water. In Fig. 1 it can be seen that at 40 $^{\circ}$ C and 17, the deliquescence point is passed for potassium formate and for potassium acetate we are very close to the deliquescence point. Therefore, it is expected that there may be water present in a mobile state. Looking at Fig. 5, at the drop in loading at the dashed line, it can be seen that when the temperature is increased both samples directly start to loose wa-ter, indicating that water present is mobile. After the dashed line, when the temperature is further increased, both samples have a second transition, probably being a crystallization transition. It is observed that this transition is at a lower temperature for potassium acetate. Potassium formate thus shows mobility in a broader temperature range. This is also observed when considering the onset of



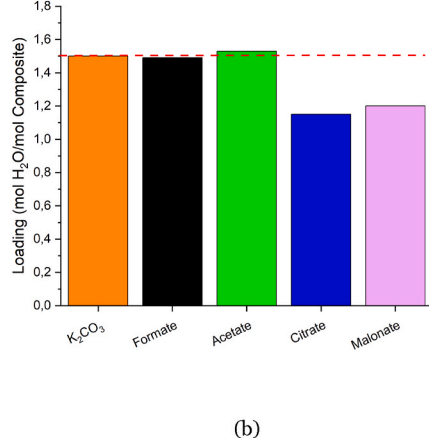


Fig. 4. Overview of the final loading reached after 20 hydration-dehydration cycles, to check the stability of the doping effect. a) per mol K_2CO_3 b) per mol composite.

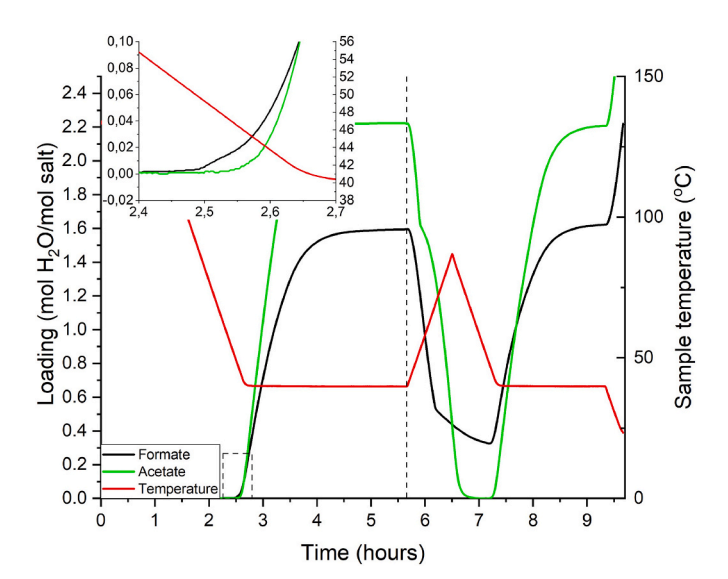


Fig. 5. Water uptake of the pure dopants; potassium-formate and -acetate at 17 mbar water vapour pressure.

water uptake, denoted by the dashed square (zoom in shown in the top left): for potassium formate onset water adsorption is 51 $^{\circ}$ C and for potassium acetate onset water adsorption 47 $^{\circ}$ C.

The same onset point screening is performed to see how the dopants effect pure K_2CO_3 . The goal is to understand how these dopants affect the hydration behaviour of K_2CO_3 . The results are shown in Fig. 6.

Initially, the sample is completely dehydrated at 140 $^{\circ}$ C. Then the tem-perature is lowered with a cooling rate of 1 K/min, at a certain temperature the samples starts to hydrate. The corresponding temperature is the onset point of hydration. Similarly, the dehydration and deliquescence points are determined, these points are plotted in the phase diagram of Fig. 7.

The onset points are shown in Fig. 7.

Looking at the hydration and dehydration onset points, there is no significant effect (taking into account the measurement error of \pm 1 $^{\circ}$ C). The metastable zone seems to be broadened slightly, indicating that, the dopants are not stimulating the nucleation. Looking at the deliquescence points, there is a significant effect. The deliquescence transition shifted from 29 $^{\circ}$ C to 38 and 39 $^{\circ}$ C for potassium-formate and -acetate respectively. This is a shift in DRH from 43 to 25 and 26% for potassium-formate and -acetate respectively.

Looking at Fig. 6 two additional observations are made. First, the

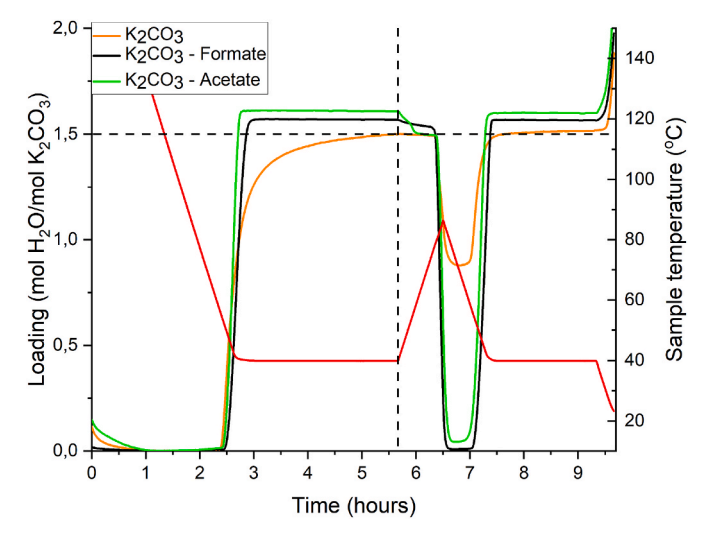


Fig. 6. Hydration, dehydration and deliquescence onset points of potassium-formate and -acetate doped K_2CO_3 and pure K_2CO_3 at 17 mbar water vapour pressure.

total water uptake is higher than that of pure K_2CO_3 . Second, part of the water present is mobile, as can be seen in the immediate drop in loading when the temperature is increased. This is in line with the observations for the pure dopants in Fig. 5.

3.2. Lattice structure and morphology

The effect of dopants on morphology is investigated to explore the impact of morphology on kinetics. The general rule is that smaller particles result in higher kinetics, due to a higher relative higher surface area. Moreover, in smaller particles more mobility is expected in the crystal lattice, increasing reaction kinetics [14]. To analyse the morphology XRD powder diffraction, SEM and BET are used.

From the XRD diffraction pattern (Fig. 8), it is seen that for all doped samples, the major peaks correspond to pure K_2CO_3 . Therefore, the crystal lattice corresponds to pure K_2CO_3 and no compounds with a different lattice are formed. Some small peaks are observed, indicating that the minor phase (i.e. the dopant) is only decorated on the surface. This is most likely, as the dopants have a higher solubility and therefore are precipitated on the surface. To analyse the surface, SEM imaging is used. K_2CO_3 , potassium-formate and-acetate doped K_2CO_3 are shown in Fig. 9.

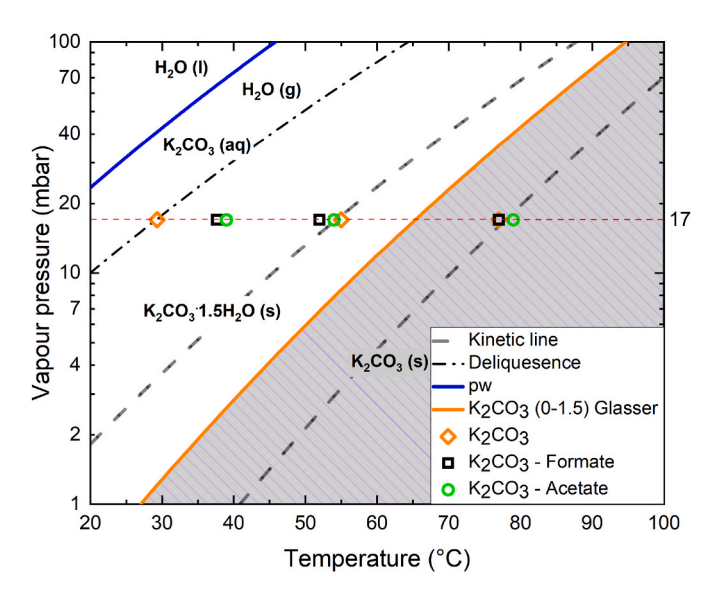


Fig. 7. Onset point screening for potassium-formate and -acetate dopants at a water vapour pressure of 17 mbar (as prepared by crystallization, content 5 mol %). From left to right the deliquescence, hydration and dehydration onset points, onset points are represented by data points.

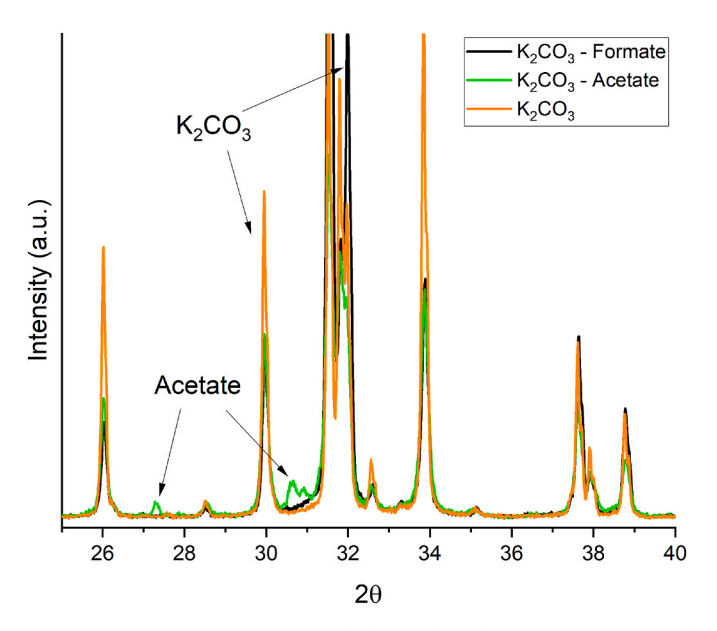


Fig. 8. Diffraction patterns of anhydrous doped-formate, -acetate and pure $K_2\mathrm{CO}_3.$

In Fig. 9 top left) a grain of pure K_2CO_3 is shown to have a smooth surface with hardly any decoration. Fig. 9 top right) shows that the formate doped sample has some surface decoration. In Fig. 9 bottom (left and right) the surface decoration can be seen more clearly. Here we have zoomed in more (5000x magnification) to have a detailed image of the sur-face composition. Both on the potassium-formate and acetate-doped sample, the grain consists of numerous smaller crystallites, increasing the overall spe-cific surface area. To quantify the surface area, BET analysis is performed. For K_2CO_3 the specific surface area is $0.29 \text{ m}^2/g$, for the formate-doped sample $0.59 \text{ m}^2/g$ and for the acetate-doped sample $2.17 \text{ m}^2/g$.

3.3. Screening the effect of crystallization on morphology

To explore if the surface area increase may be caused by the dopant

during the crystallization process, a 2D crystallization screening test is performed. This is done by mixing a saturation solution of pure $\rm K_2CO_3$ and 5 M % dopant, from which 10 ml is poured in a Petri dish. The mixed solution is evaporated under room conditions (50% RH, 21 $^{\circ}$ C). The results are shown in Fig. 10.

On the left pure K_2CO_3 is shown. The other labels indicate the dopant used in a 5 M % ratio. For pure K_2CO_3 , an overall 1D growth is observed, originating from one point in the top of the Petri dish, growing linearly from this origin.

The other (doped) samples, show a random growth of crystals. In the ac-etate sample (right), needle-like crystals are overlapping and grow in different directions, and smaller crystallites are observed. For the formate (centre), a similar observation is made, however, the needle like crystals are less defined and smaller crystallites are observed. Compared to pure K_2CO_3 both doped seem to affect the number of crystals, as has also been observed in SEM. Here only macroscopic observations can be made, for future research microscopic analyses i.e. using TEM can give more in-depth results.

3.3.1. Ionic mobility

The morphology analysis showed that the organic dopants can affect the surface area of the crystals. Kinetics can also be affected by ion mobility. The interaction with water and mobility is analysed using EIS. The experiments are performed under vacuum conditions at a sample temperature of 72 $^{\circ}$ C and vapour pressures from 16 to 66 mbar using pure-, acetate- and formate-doped potassium carbonate. The conductivity measurements are shown in Fig. 11.

In Fig. 11a, pure K_2CO_3 is shown. Due to water adsorption on the surface of a salt hydrate, the mobility and the conductivity increase, as indi-cated by the vertical arrow with increasing vapour pressure p_w [11]. Focusing on the conductivity at the highest vapour pressure (66 mbar), the conductivity increased slightly till 1×10^{-8} S/m. In Fig. 11b, the conductivity with acetate doping is shown, an increase is observed till 1×10^{-7} S/m, the width of the plateau extends here till almost 100 Hz. For acetate doping there is an effect on the conductivity, and thus mobility of water and ions on the surface.

In Fig. 11c, the conductivity for formate doping is shown. Here, the ef-fect is completely different. At low vapour pressures, a significant increase in conductivity is observed and at the highest vapour pressure, the conductiv-ity increases with 5 orders of magnitude. Moreover, the conductivity extends over the whole frequency range, indicating that water and ions are extremely mobile.

To understand the difference in mobility, a detailed measurement is per-formed on water adsorption behaviour using TGA. The measurements are performed at a 10 times lower heating and cooling rate (0.1 K/min), to ob-tain a more detailed picture on the different stages of water adsorption. The TGA results are shown in Fig. 12.

It is observed that the potassium acetate doped sample does take up more water. However, this transition occurs at a lower temperature as can be seen by the transition indicated by the indicated area a). Before this transition the potassium acetate doping must thus be present as a crystalline phase, in this phase no mobility is introduced. The second transition is probably del-iquescence. This is plausible as increasing temperature immediately reduces loading, which implies that this is mobile water.

4. Discussion

Doping with the organic salts potassium formate and potassium acetate increases the hydration kinetics of K_2CO_3 . Two different mechanisms seem to play a role here, as schematically indicated in Fig. 13; an increase in mobility due to enhanced water adsorption, by dopants with a low DRH (left), and an increase in surface area (right).

It has been shown that the deliquescence onset points are affected signif-icantly. At a cooling rate of 1 K/min, the DRH shifted from 43% for pure K₂CO₃ to 25 and 26% for formate- and acetate-doped,

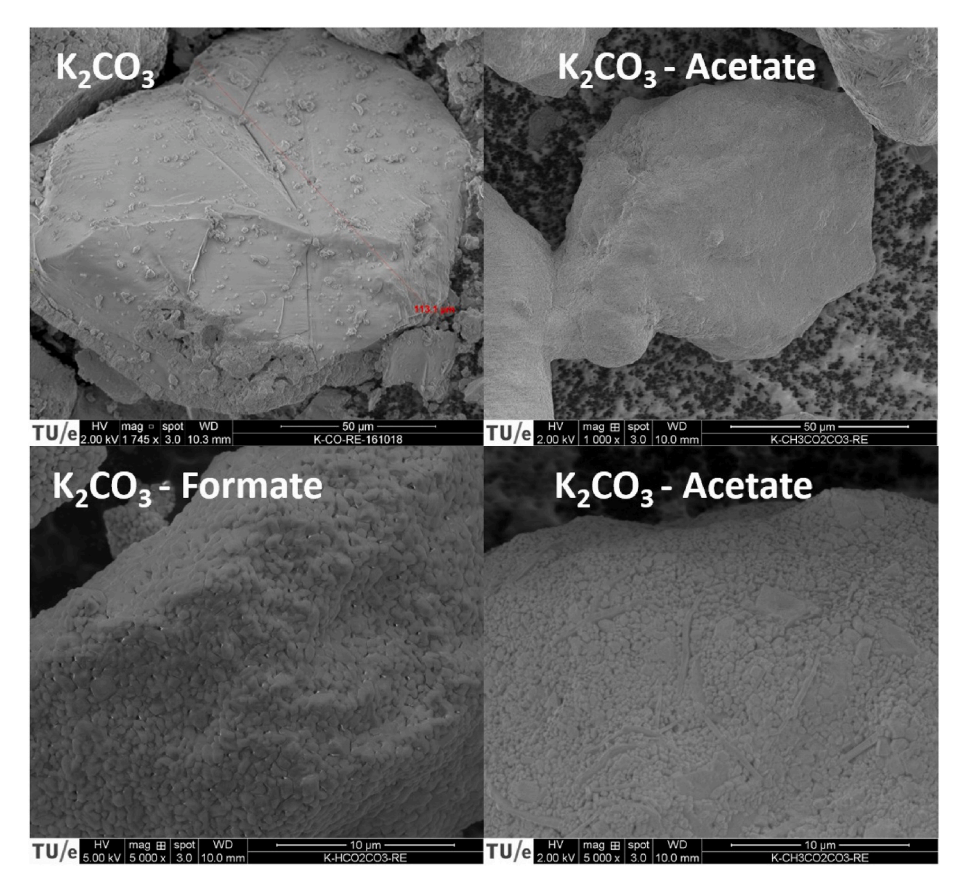


Fig. 9. Top left) Grain of K_2CO_3 scale bar. Top right) Grain of acetate-doped K_2CO_3 . Bottom left) Grain of formate-doped K_2CO_3 . Bottom right) Grain of acetate-doped K_2CO_3 . In the top a scale bar size of 50 and in the bottom a scale bar of 10 μ m.



Fig. 10. 2D crystallization test. In the center pure K_2CO_3 ; the others are 5 M % doped K_2CO_3 , with dopants as indicated by label.

respectively. This affects mobility and does enhance the hydration reaction. However, it should be noted that a lower DRH also affects the temperature operating window. Since for material stability, deliquescence should always be avoided.

5. Conclusion

This work aimed to find organic dopants to enhance the hydration kinet-ics of K_2CO_3 . Organic potassium salts have been selected based on steric compatibility having a carboxylate ion and the potential to improve mobility, which is a pre-requisite of the phase transition [11]. Since potassium-formate and -acetate increases water adsorption, this work has focused on these can-didates.

SEM and BET show that, after preparation, more surface area is present for formate and acetate doping. With formate doping the surface area only increased slightly, but with acetate doping the surface area increased 7.5 times. With XRD it has been verified that dopants have

only a morphological effect.

Besides the morphological effect, formate and acetate doping impact the water adsorption at the crystal surfaces. Looking at the pure dopants, for-mate and acetate have a DRH of 17 and 23%, respectively and it is known that below the DRH, mobility is already introduced [11].

It has been shown that the deliquescence onset points are affected significantly. At a cooling rate of 1 K/min, the DRH shifted from 43% for pure K_2CO_3 to 25 and 26% for formate- and acetate-doped, respectively. This further indicates that the dopants clearly have an effect on the water adsorption behaviour on the surface, and related to this the ion mobility on the surface. EIS showed that both potassium-formate and -acetate increases ionic mobility. Formate has a significant effect on mobility, at the highest vapour pressure, the conductivity increased by 5 orders of magnitude.

Using TGA, at a low cooling rate, it has been shown that water adsorption of the acetate dopant occurs after the hydration transition of K_2CO_3 . This may explain why the mobility is less affected by the acetate

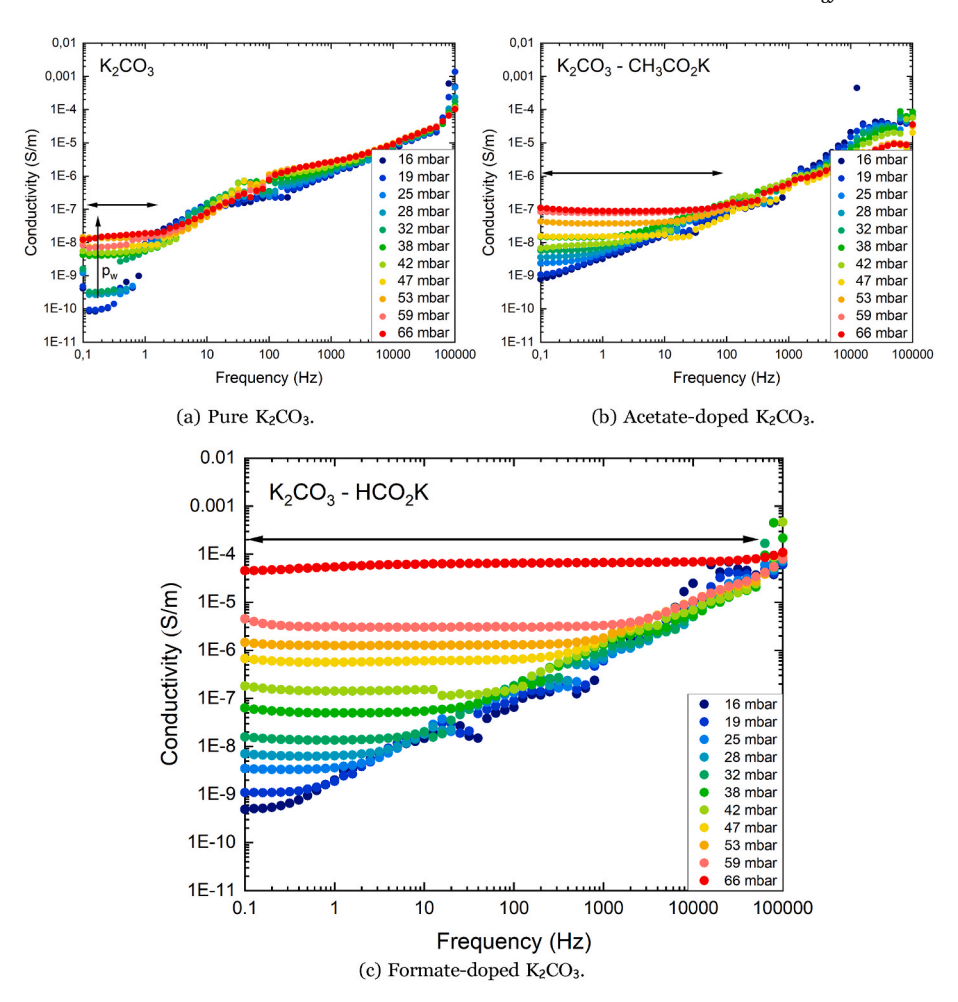


Fig. 11. Conductivity measurements of pure K₂CO₃, formate- and acetate-doped K₂CO₃ at a sample temperature of 72 °C.

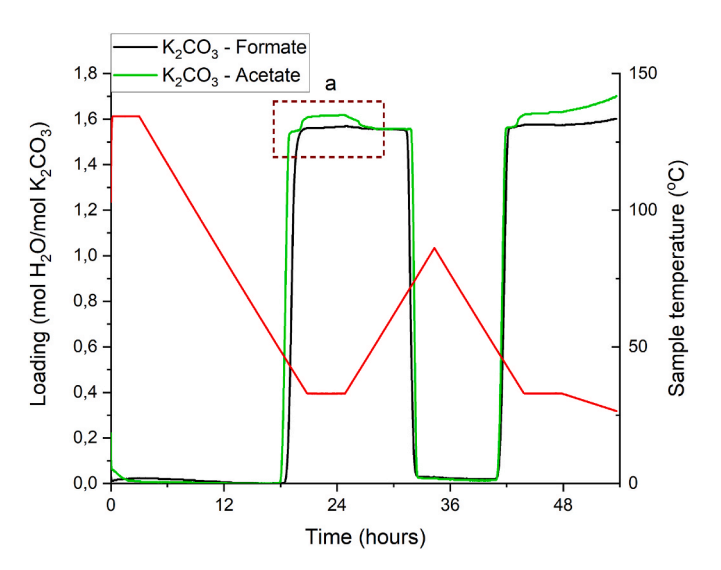


Fig. 12. Isobaric experiment at varying temperatures to screen the onset points of hydration, dehydration and deliquescence for the potassium-formate and -acetate doped K_2CO_3 . Water vapour pressure of 17 mbar and a rate of 0.1 K/min.

doping. Water adsorption on formate occurs at a lower RH, therefore, mobility seems to be present at an earlier stage. For acetate doping, both increased adsorption and increased surface area, seem to play a role in enhancing the hydration ki-netics. The water adsorption behaviour is

affected as shown by the increased water uptake and a lowering in DRH (from 43 to 26%) and the surface area increased with a factor of 7.5.

For formate doping, the major effect seems to be caused by increased mobility at the crystal surface. This was clearly supported in the EIS mea-surement. Since ionic mobility is a prerequisite for the phase transition, this increase in mobility enhances the hydration rate of $K_2\mathrm{CO}_3$.

Summarizing, organic dopants increase the hydration rate by either, in-creasing the effective surface area after preparation, or by actively adsorbing more water on the surface prior to hydration.

This work is of significant importance in the view of heat storage appli-cations. As mobility is a limiting factor for salt hydrates as K_2CO_3 , find-ing ways to enhance mobility directly increases the power output of a heat battery. Mobility can effectively be enhanced with soluble dopants such as potassium-formate and -acetate.

CRediT authorship contribution statement

Jelle Houben: Writing – review & editing, Writing – original draft, Validation, Methodology, Investigation, Conceptualization. Joris van Biesen: Investigation. Henk Huinink: Writing – review & editing, Supervision, Methodology, Formal analysis, Conceptualization. Hartmut R. Fischer: Writing – review & editing, Supervision, Methodology, Conceptualization. Olaf C.G. Adan: Writing – review & editing, Supervision, Funding acquisition.

Declaration of competing interest

The authors declare that they have no known competing financial

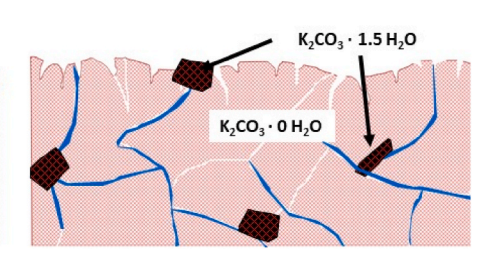


Fig. 13. On the left, hydration is accelerated by increasing the mobility on the surface due to enhanced water adsorption of the dopant. Right, the effective surface area is in-creased by reducing grain sizes. Hydration is accelerated, since more surface is introduced enhancing water adsorption is enhanced and initiating hydration.

interests or personal relationships that could have appeared to influence the work reported in this paper.

Data availability

Data will be made available on request.

Acknowledgements

This work was funded by the TKI project Dope4Heat with project number 1507201 and the Dutch Organization for Applied Research (TNO). This work reflects only the authors view. The authors thank Hans Dalderop and Jef Noijen for their technical support.

References

- [1] European, Commission, Roadmap, 2050, Policy, 2012, pp. 1–9. http://www.roadmap2050.eu/, 10.2833/10759. arXiv:ISBN 978-92-79-21798-2.
- [2] R.J. Clark, A. Mehrabadi, M. Farid, State of the art on salt hydrate thermochemical energy storage systems for use in building applications, J. Energy Storage 27 (2020), 101145, https://doi.org/10.1016/j.est.2019.101145, 10.1016/j. est.2019.101145.
- [3] K. Edem N'tsoukpoe, T. Schmidt, H.U. Rammelberg, B.A. Watts, W.K.L. Ruck, A Systematic Multi-step Screening of Numerous Salt Hydrates for Low Temperature Thermochemical Energy Storage, 2014, https://doi.org/10.1016/j. apenergy.2014.02.053.
- [4] T. Yan, T.X. Li, R.Z. Wang, Thermochemical heat storage for solar heating and cooling systems, in: Advances in Solar Heating and Cooling, Elsevier Inc., 2016, pp. 491–522, https://doi.org/10.1016/B978-0-08-100301-5.00018-7.
- [5] P.A. Donkers, L.C. Sögütoglu, H.P. Huinink, H.R. Fischer, O.C. Adan, A review of salt hydrates for seasonal heat storage in domestic applications, Appl. Energy 199 (2017) 45–68, https://doi.org/10.1016/j.apenergy.2017.04.080, 10.1016/j. apenergy.2017.04.080.

- [6] K.E. N'Tsoukpoe, H. Liu, N. Le Pierres, L. Luo, A Review on Long-Term Sorption Solar Energy Storage, 2009, https://doi.org/10.1016/j.rser.2009.05.008.
- [7] L. Luo, A review of potential materials for thermal energy storage in building applications 18 (2013) 327–349, https://doi.org/10.1016/j.rser.2012.10.025.
- [8] A. Fopah Lele, F. Kuznik, H.U. Rammelberg, T. Schmidt, W.K. Ruck, Thermal decomposition kinetic of salt hydrates for heat storage systems, Appl. Energy 154 (2015) 447–458, https://doi.org/10.1016/j.apenergy.2015.02.011, 10.1016/j. apenergy.2015.02.011.
- [9] T. Kousksou, P. Bruel, A. Jamil, T. El Rhafiki, Y. Zeraouli, Energy storage: Applications and challenges 120 (2014) 59–80, https://doi.org/10.1016/j.solmat/2013.08.015
- [10] L.C. Sögütoglu, M. Steiger, J. Houben, D. Biemans, H.R. Fischer, P. Donkers, H. Huinink, O.C. Adan, Understanding the hydration process of salts: the impact of a nucleation barrier, Cryst. Growth Des. 19 (2019) 2279–2288, https://doi.org/ 10.1021/acs.cgd.8b01908.
- [11] J. Houben, D. Langelaan, L. Brinkman, H. Huinink, H.R. Fischer, O.C. Adan, Understanding the hydration pro- cess of salts: the relation between surface mobility and metastability, Cryst. Growth Des. 22 (2022) 4906–4916. URL: http s://pubs.acs.org/doi/full/10.1021/acs.cgd.2c00416, 10.1021/ACS.CGD.2C00416.
- [12] M. Steiger, K. Linnow, H. Juling, G. Gülker, A. El Jarad, S. Brüggerhoff, D. Kirchner, Hydration of MgSO₄ · H₂O and generation of stress in porous materials, Cryst. Growth Des. 8 (2008) 336–343, https://doi.org/10.1021/ cg060688c.
- [13] N. Mazur, H. Huinink, H. Fischer, P. Donkers, O. Adan, Accelerating the reaction kinetics of K₂CO₃ through the addition of CsF in the view of thermochemical heat storage, Sol. Energy 242 (2022) 256–266. URL: https://linkinghub.elsevier. com/retrieve/pii/S0038092X22005023. URL: https://doi.org/10.1016/J. SOLENER.2022.07.023.
- [14] J. Houben, A. Shkatulov, H. Huinink, H. Fischer, O. Adan, Caesium doping accelerates the hydration rate of potassium carbonate in thermal energy storage, Sol. Energy Mater. Sol. Cell. 251 (2023), 112116, https://doi.org/10.1016/J. SOLMAT.2022.112116.
- [15] L.J. Mauer, Deliquescence of crystalline materials: mechanism and im- plications for foods, Curr. Opin. Food Sci. 46 (2022), 100865, https://doi.org/10.1016/J. COFS.2022.100865.